Endocrine, *vol. 26, no. 2, 117–125, March 2005* 0969–711X/05/26:117–125/$30.00

IGF-I and Postnatal Growth of Weaver Mutant Mice

Weiguo Yao,[1] Jin Zhong,[2] Clifford J. Rosen,[3] Janet M. Hock,[1] and Wei-Hua Lee[1,2]

Departments of Anatomy and [1]Cell Biology and [2]Pediatrics, Indiana University, IN 46202; and [3]Maine Center for Osteoporosis Research and Education, St. Joseph Hospital, Bangor, ME 04401

IGF-I is an anabolic growth factor essential for growth and development, both as a mediator of growth hormone (GH) action and as a local stimulator of cell proliferation and differentiation. Although the importance of IGF-I in postnatal growth has been studied for several decades, its functions in pathological states are not fully understood. The weaver (*wv*) mutant mouse is a commonly used model for studying hereditary cerebellar ataxia and provides us with an opportunity to study the function of IGF-I in postnatal growth during neurodegeneration. In prepubertal *wv* mice, we found a parallel decrease in body weight and serum IGF-I. This parallel relationship was maintained in females, but not in males, as *wv* mice entered puberty. Interestingly, we found an increase in the levels of circulating IGF-I and hepatic mRNA preceded the catch-up of body weight of pubertal male *wv* mice. The increase in IGF-I levels coincided with a surge of circulating androgen at the onset of male puberty, suggesting that androgen might trigger the increase in IGF-I production in the pubertal and adult male *wv* mice. Overall, our results support the concept that IGF-I plays an important role in postnatal growth during and after neurodegeneration of *wv* mice. In addition, IGF-I's regulation of systemic growth during and after puberty is likely modulated by androgen in male *wv* mice.

Key Words: IGF-I; weaver mice; growth; puberty.

Introduction

IGF-I plays an essential role in embryonic and postnatal growth of the mammalian system. The importance of IGF-I in postnatal growth is best demonstrated by genetic manipulation in mice. Most mice with IGF-I null mutation die; those who survive have low birth weight (60% of wild-type littermates) and exhibit severe postnatal growth retardation with body weight only 30% of that of their wild-type littermates at 2 mo of age *(1,2)*. Conversely, mice overexpressing the IGF-I gene demonstrated a small but significant (approx 1.4-fold) increase in body weight, starting around 2 mo postnatally *(3,4)*. IGF-I's growth promoting action is predominantly under the regulation of growth hormone (GH). GH receptor (GHR) knockout mice lack response to GH and their plasma IGF-I level is reduced by 90%, while body weight is reduced to 50% of that of wild-type littermates (*5*). In GH transgenic mice, circulating IGF-I increased by about two- to threefold, and body weight increased by twofold, compared to their wild-type littermates *(6,7)*. Collectively, these observations establish the fundamental importance of the GH/IGF-I axis in systemic growth and development.

IGF-I is produced in many tissues, and acts as a paracrine/autocrine growth factor for the differentiated functions of many organs, including the CNS *(8)*. Although the role of GH/IGF-I in normal growth of rodents has been established, its growth-promoting function in pathological states, such as genetic mutation–induced neurodegeneration, has not been investigated. Weaver (*wv*) mice have been used as a model to study neuropathogenesis of cerebellum ataxia *(9,10)*, which is primarily due to the premature apoptosis of cerebellar granule neurons. Our previous work showed *wv* granule neurons overexpress IGF binding protein 5 (IGFBP5), one of six IGFBPs, just before they died *(11)*. Because IGFBP5 interferes with the interaction between IGF-I and IGF-IR, excess IGFBP5 may accelerate granule cell apoptosis. Exogenous IGF-I or des(1-3) IGF-I partially rescued *wv* granule neurons from undergoing apoptosis in vitro *(12)*. During the course of our investigation, we found *wv* mice grow poorly even on wet feed, which was intended to help the mice obtain enough water and nutrients to support their growth. Previously, a reduced hepatic IGF-I synthesis and circulating IGFI levels were implicated in the poor growth of another line of cerebellar ataxic mice, Purkinje cell degeneration mice *(13,14)*. Interestingly, a decrease in serum IGF-I levels was also reported in human neurodegenerative diseases *(15,16)*. These observations prompted us to study the role of IGF system genes in the postnatal growth of *wv* mice.

In this investigation, we first characterized the growth pattern of *wv* mutant mice. In parallel, we measured circulating IGF-I and hepatic IGF-I mRNA expression to determine correlation with systemic growth patterns. Because the

Received November 29, 2004; Revised February 4, 2005; Accepted February 10, 2005.

Author to whom all correspondence and reprint requests should be addressed: Dr. Wei-Hua Lee, Riley Research, Rm 208, 699 West Drive, Indiana University Medical Center, Indianapolis, IN 46202. E-mail: whlee@iupui.edu

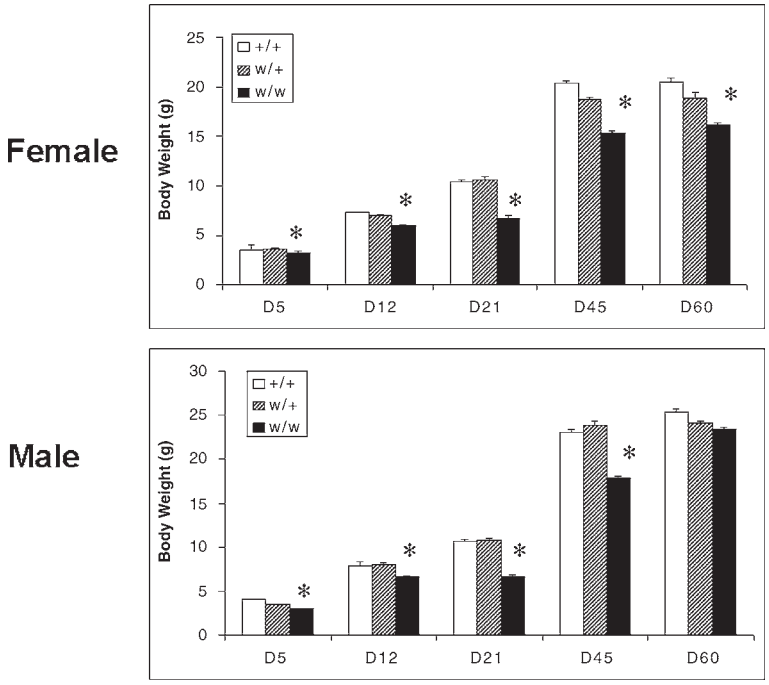

Fig. 1. Body weights of +/+, *w*/+ and *w*/*w* mice of female or male at P5, 12, 21, 45, and 60. Data are expressed as means ± SEM. ($n = 6$). *$p < 0.05$ compared with mean weights of age-matched +/+ mice, as assessed by one-way ANOVA.

biological activity of IGF-I is closely associated with the levels of IGFBPs in the circulation, we measured levels of IGFBPs in the same sample, and determined hepatic IGFBP3 mRNA and protein, the major IGFBP that forms complexes with IGF-I in the circulation. Our results implicate IGF-I in the poor growth of *wv* mice during early postnatal period. With the onset of puberty, growth was restored in male but not in female, *wv* mice, suggesting a gender bias that most likely involves the differential regulation of IGF-I by androgens in males.

Results

Postnatal Body Growth of Weaver Mice

Weaver mice grow poorly during their postnatal life, especially in the first month. At postnatal d 21, both male and female homozygous *wv* mice showed body weight gain that was two-thirds that of their wild-type littermates (65% and 68% respectively, Fig. 1). Decreases at this magnitude were already seen soon after birth at postnatal d 5, suggesting that systemic growth is retarded prior to birth, during embryonic life. After the onset of puberty, a gender difference in systemic body growth of *wv* mice started to emerge. While female *wv* mice continued to grow poorly in their postnatal life, male *wv* mice increased their body weights and caught up from a deficit of 22% at d 45 to within 8% of wild-type littermates at postnatal d 60 (Fig. 1). In contrast, the body weights of female homozygous *wv* mice remained at approx 78% of their wild-type littermates between postnatal d 45 and 60. Besides comparing the difference among genotypes within age and sex with one-way ANOVA, we also used DOE to evaluate the age-related alterations, sex effects, and potential interactions between these factors. DOE analysis suggested that age, gender, interactions between genotype and age, and the interactions between age and gender all have significant effects on body growth of *wv* mice, and the p values are $p < 0.001$, $p < 0.001$, $p < 0.05$, and $p < 0.001$, respectively.

Levels of Circulating IGF-I and Hepatic IGF-I mRNA in Weaver Mice

Our previous work showed that a decrease in IGF-I activity contributes to the premature apoptosis of granule neurons in the *wv* cerebellum *(12)*, which is the primary cause of their ataxic phenotype. Because the IGF-I/GH axis plays an important role in postnatal growth, we measured total IGF-I circulating levels in the same group of mice whose body weights were measured on postnatal d 21, 45, and 60. In general, circulating IGF-I levels were between 100 and 400 ng/mL, which agrees with published data *(17)*. As shown in Fig. 2, the order of serum IGF-I levels in three genotypes of *wv* mice follow the order of their body weights, especially in female homozygous *wv* mice ($r^2 = 0.95$ in regression analysis). At all three postnatal dates, serum IGF-I

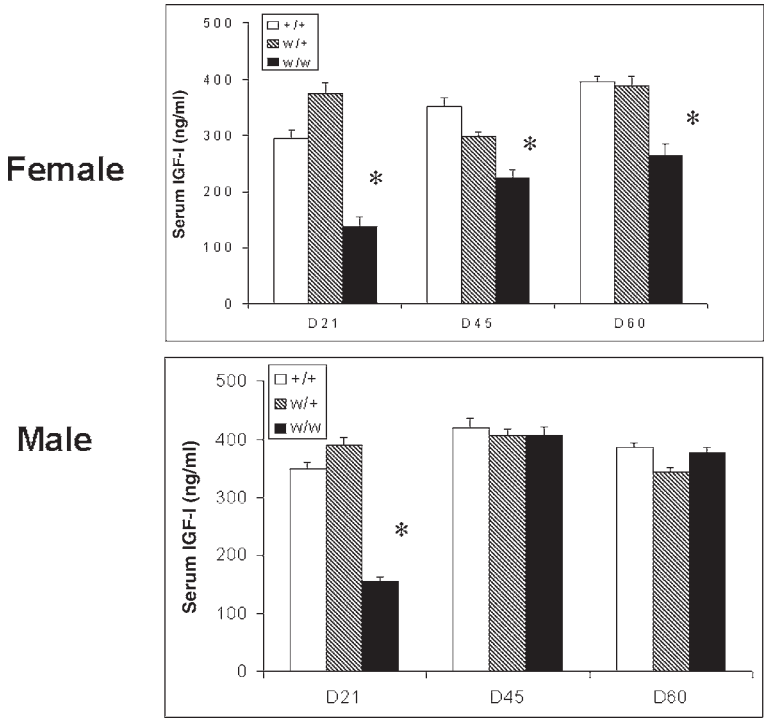

Fig. 2. Serum IGF-I levels of +/+, *w*/+, and *w*/*w* mice of both genders at P21, 45, and 60. Serum IGF-I levels were measured by radioimmunoassay. Each value represents means ± SEM. ($n = 5–6$). *$p < 0.05$ compared with mean serum IGF-I levels from age-matched +/+ mice, as assessed by one-way ANOVA.

levels were the lowest in female homozygous *wv* mice and the highest in their wild-type littermates. At postnatal d 21, serum IGF-I levels in homozygous *wv* mice were less than half of their wild-type littermates in both females (–54%) and males (–55%). As male *wv* mice entered puberty, serum IGF-I levels increased to equal the IGF-I levels of their wild-type littermates (Fig. 2). While this trend was maintained at P60 in males, serum IGF-I remained approx 65% between d P45 to P60 In female *wv* mice (Fig. 2). These data show that the gender-dependent switch in IGF-I levels and body growth of *wv* mice was observed at the onset of puberty. Besides comparing the difference among genotypes within age and sex with one-way ANOVA, DOE analysis on the age-related alterations, sex effects, and potential interactions between these factors suggested that age, gender, the interaction between genotype and age, and the interaction between age and gender all have significant effects on body growth of *wv* mice, and the *p* values are $p < 0.001$, $p < 0.001$, $p < 0.001$, and $p < 0.01$, respectively.

Because most circulating IGF-I is synthesized and released from the liver, we examined hepatic IGF-I mRNA expression in the same group of *wv* mice. Within the three mRNA species identified on Northern blot analyses (7.5, 1.3, and 0.6–1 kb), the small-molecular-weight (0.6–1.0 kb) band was most abundant in all age groups (Fig. 3A). We analyzed the optical density on film autoradiograph to estimate levels of this mRNA species in all three genotypes of male and female *wv* mice (Fig. 3B). Like circulating IGF-I, hepatic mRNA expression was the lowest in female *wv* mice of all three postnatal ages, and paralleled the decrease in circulating IGF-I levels. For unknown reasons, hepatic IGF-I mRNA levels are the highest (approx 35% higher that their wild-type littermates) in heterozygous *wv* mice on postnatal d 21 for both male and female *wv* mice. Hepatic IGF-I mRNA expression in male mice at postnatal d 45 increased to the level of their wild-type littermates. This increase coincided with the increase in their circulating IGF-I levels, implicating the liver as the source of increased circulating IGF-I during male puberty. DOE analysis suggested that age, the interaction between age and gender, and the interaction among genotype, gender, and age, all have significant effects on body growth of *wv* mice and the *p* values are $p < 0.001$, $p < 0.001$, and $p < 0.05$, respectively.

Levels of Circulating IGFBPs and Hepatic IGFBP3 in wv *Mice*

The levels of circulating IGF-I are normally regulated by circulating IGFBPs, which not only transport IGFs to their target organs but also protect IGFs from proteolysis *(18)*. To study the potential involvement of IGFBPs in regulating circulating IGF-I levels, we employed a ligand blot method to measure IGFBPs, which were estimated by optical density analysis *(19)*. As shown on Fig. 4A, the dominant circulating IGFBPs were IGFBP2 and -3, consistent with

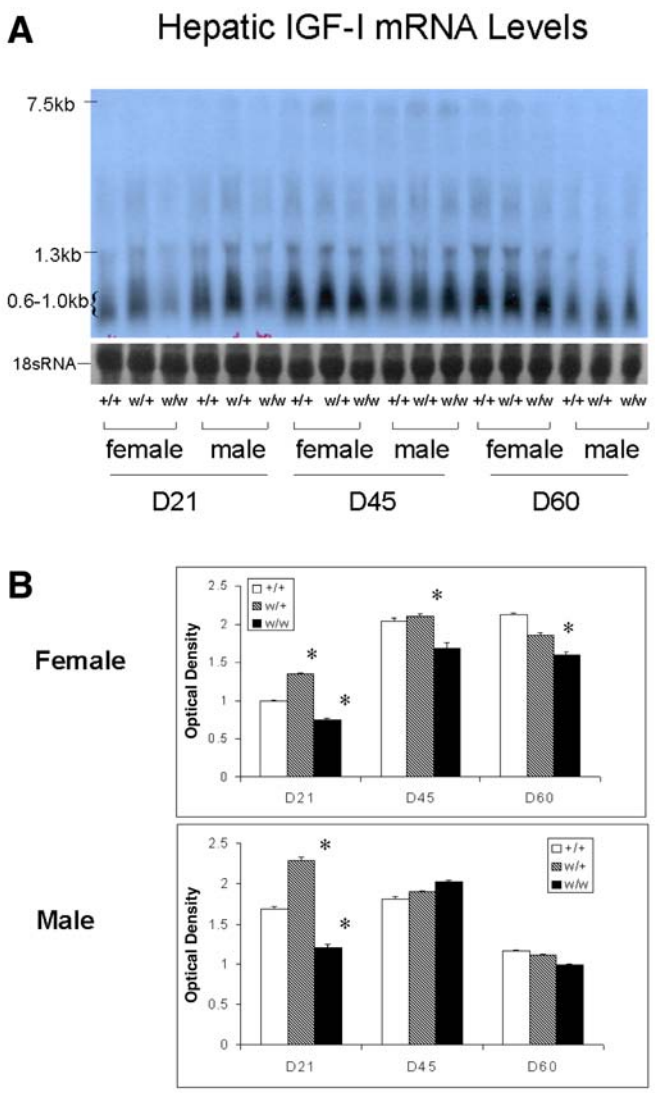

Fig. 3. Hepatic IGF-I mRNA levels in +/+, *w*/+, and *w*/*w* mice of both genders at P21, 45, and 60. (**A**) IGF-I mRNA levels were measured in total hepatic RNAs by Northern blot hybridization. For each sample, three major bands of hepatic IGF-I mRNA (size 0.6–1.0 kb, 1.3 kb, and 7.5 kb) were detected. The lower panel shows the quality and evenness of sample loading by ethidium bromide staining of the 18S on the agarose gel used for the same Northern blot. The figure is a representative of all the data. (**B**) Changes in the hepatic IGF-I mRNA (0.6–1.0 kb) levels of three genotype mice at different developmental stages were quantified by densitometry analysis of autoradiography, within a linear range. Each value represents means ± SEM ($n = 6$). *$p < 0.05$ compared with the mean IGF-I levels in age-matched +/+ mice, as assessed by one-way ANOVA.

published work *(19)*. The circulating IGFBP3 levels were decreased in female weaver mice and D21 male weaver mice, compared to their age-matched wild-type littermates. But in D45 and D60 male weaver mice, IGFBP3 caughtup to normal level (Fig. 4B). In contrast to IGFBP3, circulating IGFBP2 maintained at normal levels in both male and female weaver mice, except in D21 male weaver mice, which showed a decreased IGFBP2 level for unknown reasons (Fig. 4C). These results suggested that there may be a coordinate regulation of circulating IGF-I and IGFBP3. DOE analysis on IGFBP3 suggested that age, the interaction between age and gender, and the interaction among genotype, gender, and age, all have significant effects on body growth of *wv* mice and the *p* values are $p < 0.001$, $p < 0.001$, and $p < 0.05$, respectively.

Most IGFBP3 is circulating in the 150 kDa complex, which consists of IGF-I, IGFBP3, and ALS. To see if there was a coordinated decrease in IGFBP3 expression, we measured IGFBP3 mRNA expression by RT-PCR in total mRNA collected from the same groups of mice. As shown in Fig. 5A, there was no difference in IGFBP3 mRNA levels among all genotypes and genders. To determine if potential post-translational modification affected IGFBP3 protein levels, we examined IGFBP3 protein expression in liver, using Western immunoblotting. As shown in Figs. 5B and 5C, there was no significant difference in IGFBP3 expression in the liver, suggesting that IGFBP3 production is not affected by the *wv* mutation and, therefore, is unlikely to be involved in regulation of IGF-I circulating levels. DOE analysis suggested that age, gender, and potential interactions between these factors have no significant effects on hepatic IGFBP3 levels.

Discussion

As essential regulators for the systemic body growth, maintaining the integrity of the GH/IGF-I axis is important in a variety of pathological states, especially if IGF-I may be involved. This investigation studied the role of IGF-I during and after neurodegeneration, using *wv* mutant mice as an animal model. Previously, decreased IGF-I neurotrophic activity was implicated in the premature apoptosis of cerebellar granule neurons *(12)*. We now report that circulating IGF-I decreased in *wv* mice, and the decrease was observed in parallel to the failure of *wv* mice to gain body weight in early postnatal life. This parallel relationship was maintained in females, but not in males as *wv* mice enter puberty. Interestingly, we found an increase in circulating IGF-I levels and hepatic IGF-I mRNA expression preceded the increase in body weight of pubertal male *wv* mice, suggesting androgen surge at the onset of puberty may be responsible for this catch-up body weight gain.

First described in 1964 *(20)*, the weaver mutant mouse is characterized by ataxia, hyperactivity, and tremor *(21, 22)*. The ataxic phenotype is linked to the depletion of granule neurons in the cerebellum, although other brain regions, such as the hippocampus and midbrain, as well as testis, are also abnormal *(23,24)*. In the present study, homozygous *wv* mice grew poorly, especially in the prepubertal period. At the time of weaning (P21), body weight gain of male and female homozygous *wv* mice was approx 35% less than their

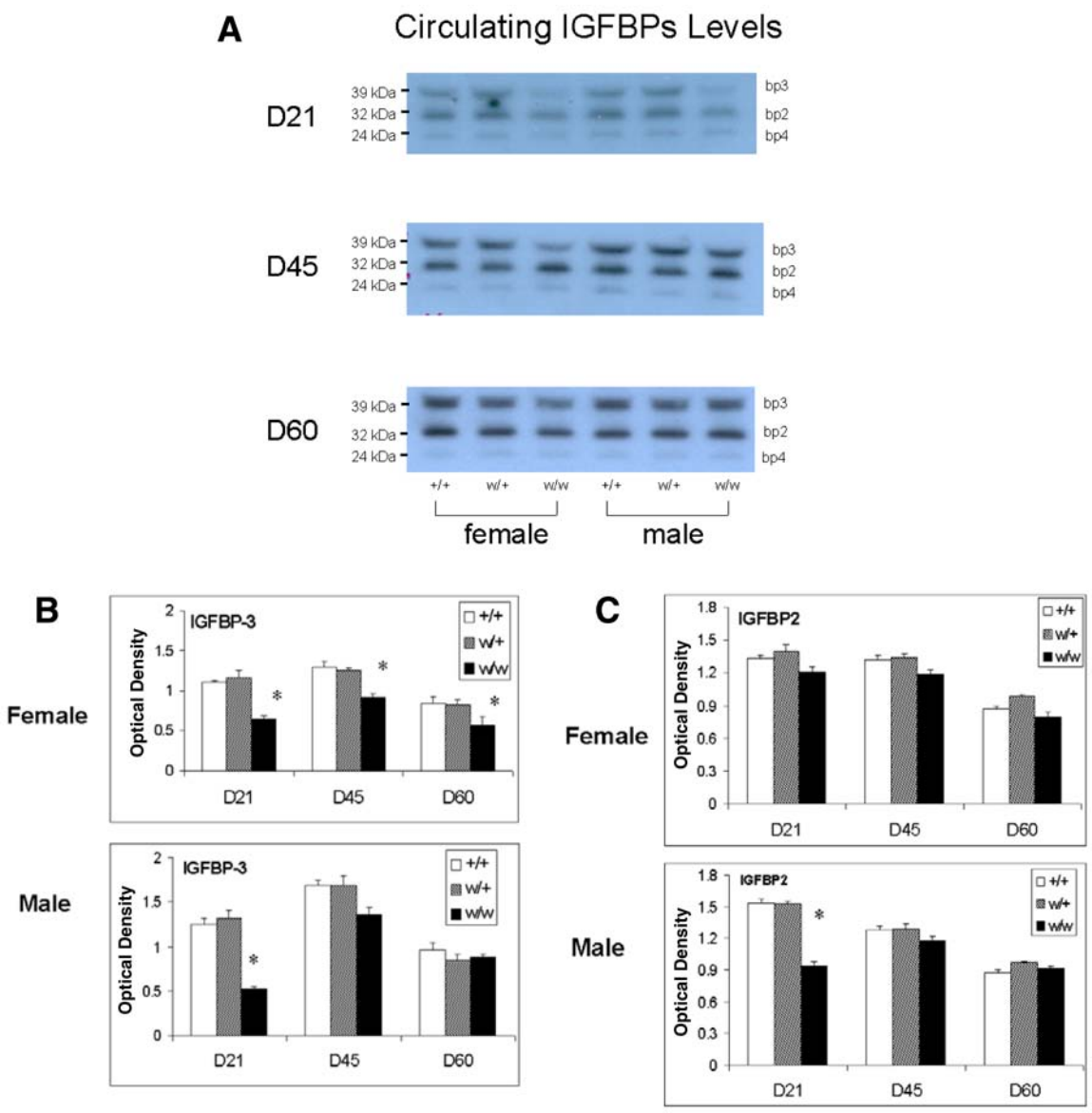

Fig. 4. Serum IGFBPs in +/+, *w*/+, and *w*/*w* mice of both genders at P21, 45, and 60. The profiles of serum IGFBPs levels were measured by Western ligand blot. Each IGFBP was quantified by densitometry analysis of autoradiograph, on which IGFBPs-3 (MW: 39 kDa), -2 (32 kDa), and -4 (24 kDa) were detected (**A**). The figure is a representative of all the data. Changes in circulating IGFBP-3 (**B**) and -2 (**C**) of three genotype mice at different developmental stages were within the linear range of the optical density. Each value represents mean ± SEM ($n = 6$). *$p < 0.05$ compared with age-matched +/+ mice, as assessed by one-way ANOVA.

wild-type littermates. In fact, body weight of *wv* homozygous mice was already substantially lower than wildtype controls at P5, the earliest time point we could obtain their genotypes. Because *wv* mice are not ataxic at P5, the failure in systemic growth was likely initiated during embryogenesis, when IGF-I is known to be an important growth factor *(1)*. In puberty (P45), body weight gain of male and female homozygous *wv* mice lagged compared to wild-type littermates. Despite the severe ataxia, the body weight gain of male adult (P60) homozygous *wv* mice accelerated during puberty, while those of females did not, suggesting nutritional factors do not play a major role, instead, a gender-related switch was turned on at the onset of male puberty.

Puberty marks the transition from childhood to adulthood in terms of growth and reproductive maturity. Gonadotropic and somatotropic axes are activated as demonstrated by the amplification of pulsatile hormonal levels in the circulation *(25)*. During normal human puberty, androgen and estrogen increase GH production, but the feedback amplification of GH production is mainly by estrogen, even in males *(25)*. There was a significant decrease in GH production rates in prepubertal boys who were treated with an

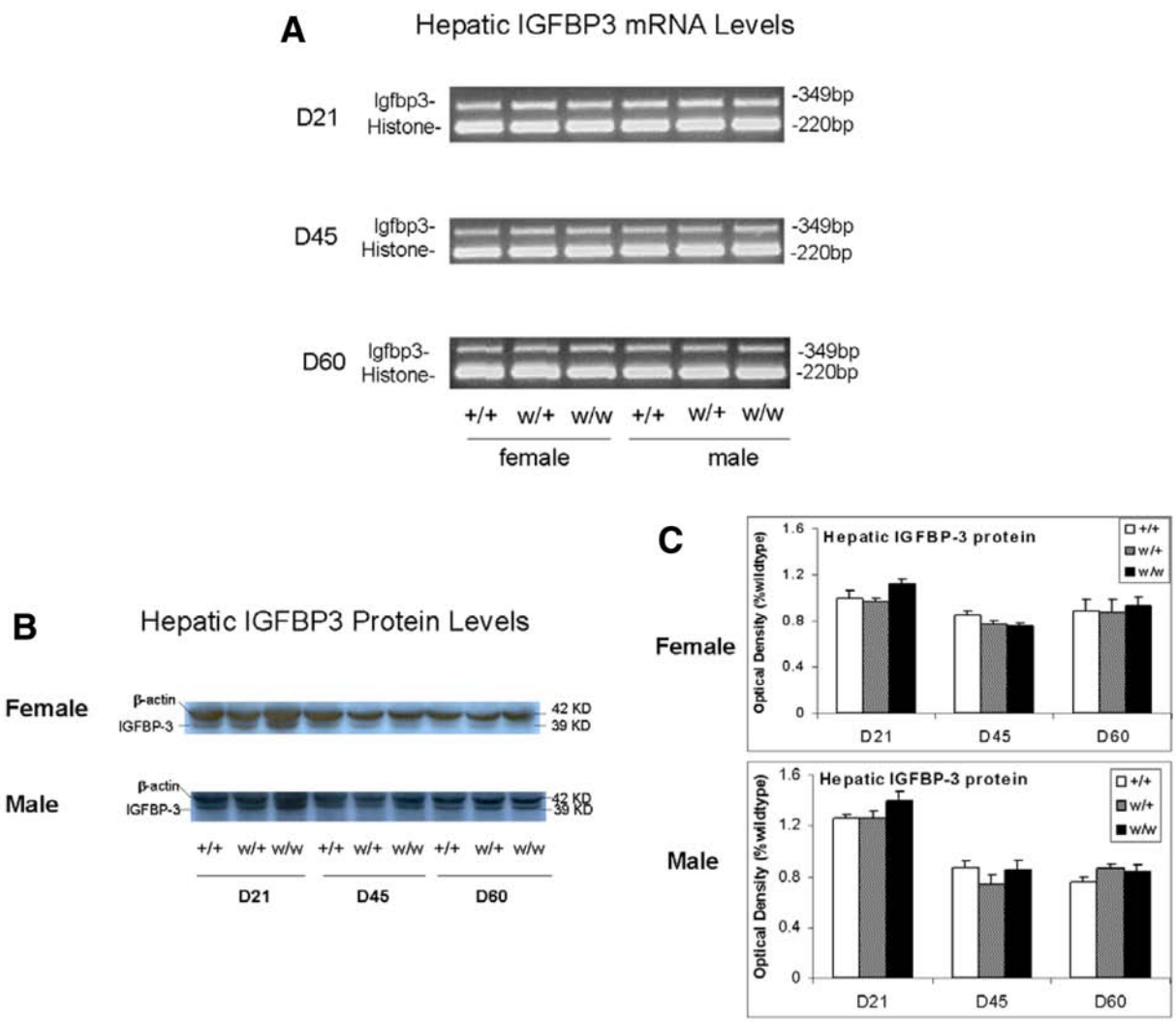

Fig. 5. Hepatic IGFBP-3 mRNA and protein levels in +/+, *w*/+, and *w*/*w* mice of both genders at P21, 45, and 60. (**A**) Hepatic IGFBP-3 mRNA levels were measured by semiquantitative RT-PCR and corrected for Histone expression. Each sample represents pooled sample ($n = 6$) from the same gender, age, and genotype mice. No significant difference was found among different gender and genotypes. The figure is a representative of all the data. (**B**) Hepatic IGFBP-3 protein levels were measured by Western blot. Total hepatic protein was run on 8% SDS-PAGE. Western blot identified the IGFBP-3 at molecular mass of 39 kDa. β-actin (42 kDa) was used to monitor the protein loading. The figure is a representative of all the data. (**C**) Changes in the hepatic IGFBP-3 protein levels were quantified by optical density on autoradiographic film, within a linear range. Each value represents means ± SEM ($n = 6$). *$p < 0.05$ compared with the mean IGFBP3 levels in age-matched +/+ mice, as assessed by one-way ANOVA.

estrogen receptor blocker (tamoxifen) *(26)*. Whether rodent gonadotropic and somatotropic axes mimic those of humans is unknown. By P60, no genotype-dependent difference was reported in serum and pituitary FSH/LH levels in female *wv* mice or in serum and testicular testosterone levels in male *wv* mice *(27)*, indicating that both female and male *wv* mice have a normal surge of sex hormones in early puberty. Despite the normal pubertal increase of sex hormone in female *wv* mice, neither their circulating IGF-I nor their body weight gain reach those of their wild-type female littermates.

By comparison, male *wv* mice demonstrated an accelerated body growth that was preceded by an increase in circulating IGF-I at P45, which stayed elevated at least to P60. Given IGF-I's role in promoting normal body growth, this sequential event suggested that the increased circulating IGF-I may be responsible for the phenomenon of catch-up systemic growth in pubertal male homozygous *wv* mice, which, we speculated, was triggered by a surge in androgen at the start of puberty. Biological effects of androgen are mediated through either direct interaction with androgen receptors or, after aromatization to estrogen, indirect action with estrogen receptors *(28,29)*. In humans, testosterone administration to elderly men increases skeletal muscle strength and protein synthesis *(30)*. This effect is likely mediated through the androgen and not the estrogen recep-

tor because nonaromatizable androgen dihydrotestosterone did not affect GH production *(31,32)*. On the other hand, infusion of rhIGF-I to young adults enhanced whole body protein anabolism *(33)*. Although how androgen regulate IGF-I synthesis in mice may differ from that of human, our observation of increased circulating IGF-I and hepatic mRNA expression in pubertal male *wv* mice supports the hypothesis that androgen may increase systemic body growth by directly regulating IGF-I synthesis in the liver and, perhaps, in peripheral tissues.

One possibility for the increase in circulating IGF-I is a decrease in IGF-I degradation, which may occur if IGFBPs is in excess. While most circulate as bound forms with IGF binding proteins (IGFBPs), the circulating IGF-I consists of three pools *(34,35)*. About 70–80% of the IGFs circulate in large complexes (150 kDa), which consists of IGFBP3 and the acid liable subunit *(36)*. About 20–25% of the IGFs are bound to other IGFBPs (IGFBP1, -2, -4, -5, and -6). Less than 1% of circulating IGF-I exists as free form. Because it can be readily translocated from the vascular compartment into target tissues, this pool of IGF-I is most important for IGF-I's biological actions *(34)*. The important role of free IGF-I in regulating postnatal growth is supported by evidence from liver-specific IGF-I knockout mice, where body growth as well as free IGF-I levels remained normal even though circulating IGF-I reduced to 25% of normal levels *(37-39)*. In pubertal male homozygous *wv* mice, the increased circulating IGF-I concentration is not likely a result of increased IGFBP circulating levels. The alteration of circulating IGFBP3 levels parallels to the alteration of circulating IGF-I levels, while circulating IGFBP2 levels maintain at normal except D21 male *wv* mice. If there are any effects, the lower levels of IGFBP3 are likely to further decrease circulating IGF-I, as occurs in female but not male *wv* mice. It is also possible that the decrease in IGFBP-3 circulating levels were secondary to the decreased serum IGF-I, which required lower IGFBP3 levels to form the IGF–BP3–ALS complex. In either case, genotype, gender, or age has no impact on hepatic IGFBP3 mRNA and protein levels, suggesting that *wv* gene mutation does not alter the transcription and translation of IGFBP3. So the decrease in circulating IGFBP3 levels in female and D21 male weaver mice may be due to the high proteolytic activity in these mice. This needs to be further studied.

In summary, our investigation has increased our knowledge of the importance of IGF-I during postnatal growth of *wv* mice, a model of hereditary cerebellar ataxia. In female *wv* mice, estrogen secretion does not alleviate the poor growth or IGF-I synthesis and release in homozygous *wv* mice. On the other hand, a direct androgen-mediated increase in hepatic and circulating IGF-I may stimulate catch-up growth in male *wv* mice. This important observation gives us insight into IGF-I's role during postnatal growth, especially in neurodegeneration such as cerebellar ataxia.

Materials and Methods

Animal and Tissue Preparation

The care and maintenance of the mice were in strict accordance with the NIH Guide for the Care and Use of Laboratory Animals. Animals were obtained from a colony of mice maintained at the Indiana University Medical Center. This colony was established from mice heterozygous for the *wv* gene purchased from the Jackson Laboratory (Bar Harbor, ME). Mutant and wild-type mice were maintained on a hybrid B6CBA-$A^{W\text{-}J}$/A stock. Homozygous *wv* mutants (*wv/wv*) were obtained by crossing pairs of heterozygous or homozygous females with heterozygous males. Animals were provided with food and water *ad libitum* and placed on a 12:12 h light/dark cycle. Mice were housed two per cage with the same genotype. Wet-feed was always provided to *wv* mice to help their feeding.

Genotyping

A point mutation of the K^+ ion channel (*Girk2) (40)* is associated with the *wv* mutation *(41,42)*. For *Age*I restriction enzyme digestion, the DNA was amplified in a 25 µL reaction volume using primers *Age*I-1 (5'-GCTTTTTTATTCT CCATAGAGACAGAAACCACCACC) and *Age*I -2 (5'-AACACGGACTGGATTAAGAAG). The *Age*I primer has a C at the penultimate base of the 3' end instead of a T, which would normally be present in genomic DNA. In the final amplification product, this results in the loss of an *Age*I site if the *wv* mutation is present. The cycling parameters are denaturation at 95°C for 2 min, followed by 35 amplification cycles (30 s at 95°C, 30 s at 66°C, 1 min at 72°C), and a final extension at 72°C for 5 min. After amplification, 10 µL of PCR products were digested with *Age*I in a 20 mL volume and evaluated by electrophoresis in an 8% polycarylamide (TBE) gel. The resulting restriction fragments were determined for mutant and normal alleles.

Western Ligand Blot

Mice serum samples (1.6 µL) were subjected to nonreducing discontinuous SDS-PAGE on a 4.0% stacking gel and 12% polyacrylamide separating gel for 45 min at 200 V. The proteins were transferred onto nitrocellulose membranes with a Bio-Rad transfer unit at 100 V for 1–1.5 h. The nitrocellulose membranes were washed with Blocking Buffer I (10 m*M* Tris, 150 m*M* NaCl, 0.05% NaN_3, 0.1% BSA, 3% Nonidet P-40, pH 7.5) for 30 min. The membranes were then washed with Blocking Buffer II (10 m*M* Tris, 150 m*M* NaCl, 0.05% NaN_3, 0.1% BSA, 0.1% Tween-20, pH 7.5) for 2 h and then rinsed in RIA buffer. The membranes were incubated *(43)* with 1 µCi of IGF-II mixed in 5 ml RIA buffer at 4°C overnight. The membranes were then washed in RIA Buffer (50 m*M* Na_2PO_4, 0.1% NaCl, 0.1% EDTA, 0.1% NaN_3, 0.02% protamine sulfate, 0.05% Tween-20, pH 7.5) and air-dried before exposure to X-ray film (Kodak) with intensifying screens at –70°C for

3 d. IGF-II was employed as the ligand because of its high affinity to all IGFBPs *(19)*. The Western ligand blot was repeated two times from the same tissue sample, and the results were reproducible. The identity of each of the IGFBP was confirmed by blotting similar membranes with antibodies against different IGFBPs (Upstates Technology). Unfortunately, the antibody made against recombinant human IGFBP4 did not cross-react with that in mice.

Western Blot

Total proteins were extracted from fresh liver by homogenization in a lysis buffer (50 m*M* PIPES, 50 m*M* KCl, 5 m*M* EGTA, 2 m*M* $MgCl_2$, and 1 m*M* DTT) and centrifuging for 10 min at 15,000*g* at 4°C. Proteins in the supernatant were separated on an 8% PAGE SDS gel and then transferred to PVDF membrane according to standard protocols. The membranes were blocked with 5% nonfat milk in TBST for 1 h at room temperature. The blots were then incubated with a rabbit polyclonal antibody against IGFBP 3 (1:1000; Cell Signaling) overnight at 4°C. After washing in TBST three times, the blots were incubated with goat anti-rabbit peroxidase-conjugated secondary antibodies at 1:2000 dilution, and the results were visualized by ECL.

RNA Preparation

Total RNA was prepared by the RNAzol™ B method, modified from the acid guanidinium thiocyanate–phenol–chloroform extraction method *(44)*. Briefly, 100 mg of frozen liver was homogenized in 2 mL of RNAzol™ B solution (Tel-Test Inc., cat. no. CS-105), vigorously mixed with 0.2-mL chloroform, cooled 5 min on ice, and then centrifuged at 12,000*g* 4°C. The aqueous layer was transferred to a new tube, mixed with an equal volume of isopropanol, stored at 4°C for 15 min, and then centrifuged at 12,000*g* for 15 min at 4°C. After centrifuging, the RNA pellet was washed in cold 75% ethanol and then dissolved in diethylpyrocarbonate-treated water, and stored at –80°C.

Northern Blot Hybridization

Total RNA (10 µg) was electrophoresed on a 1.2% agarose–formaldehyde gel at 20–25 V overnight. Photographs of the ethidium bromide–stained gel were taken under UV light. The quality and quantity of the 18S and 28S was used to assess the RNA integrity (data not shown) and 18S rRNA was used to normalize the even loading (Fig. 3). Separated RNA was transferred overnight onto nitrocellulose membranes by capillary transfer in 20X SSC overnight, then they were cross-linked to the membranes by exposure to UV light. Membranes were prehybridized (50% formamide, 0.4 *M* Na_2PO_4, 1 m*M* EDTA, 5% SDS, and 1% BSA, pH 7.2) for 1–2 h at 42°C and then probed with a ^{32}P-cDNA probe labeled with Random primer DNA labeling kit (Invitrogen, cat. no. 18187-013). The cDNA template was a 362 bp PCR product amplified from the RT product of the total mouse hepatic RNA:

Forward: 5'-ttc aca tct ctt cta cct ggc-3'
Reverse: 5'-tct tgt ttc ctg cac ttc ct-3'

The membranes were incubated at 42°C overnight, then washed sequentially in 2X SSC, 1% SDS, 0.1X SSC, 1 m*M* EDTA, and 0.5% SDS; all at room temperature. Buffer used in the final two washes consisted of 0.1X SSC, 1 m*M* EDTA, and 0.5% SDS for 30 min at 70°C. The membranes were then air dried, exposed to X-ray film at –80°C for 2 wk, and analyzed using scanning densitometry. The Northern hybridization was performed two times starting from different RNA extraction of the same tissue sample, and the results were reproducible.

RT-PCR

Total RNA was prepared by an RNAzol method according to manufacturer's instructions. A 20 µL RT reaction system contained 1 µL of sample (1 µg of total RNA), 1 µL polydT, 9 µL DEPC water, 4 µL of 5X synthesis buffer, 1 µL of 10 m*M* dNTP, 2 µL of 0.1 *M* DTT, 1 µL reverse transcriptase SuperscriptII (Invitrogene), and 1 µL RNase inhibitor. Primer sequences are as follows:

IGFBP3 (349 bp):
- Forward primer: 5'-3': AAT GCT GGG AGT GTG GAA AG
- Reverse primer: 5'-3': AGC TCT GCT TTC TGC CTT TG

Histone 3.3 (220 bp):
- Forward primer: 5'-3': GCAAGAGTGCGCCCTCT ACTG
- Reverse primer: 5'-3': GGCCTCACTTGCCTCCT GCAA

The reaction was carried out at 42°C for 50 min; then, 70oC for 10 min to denature reverse transcriptase. A 25 µL PCR reaction mixture contained 1 U DNA polymerase Tfl (Invitrogene), 2.5 µL of 10X synthesis buffer, 2.0 µL of 25 m*M* $MgSO_4$, 0.5 µL dNTP, 1.0 µL primer, respectively, 2.5 µL RT product, and DEPC water. Denature temperature was set at 94°C, annealing T_m 59°C and extending T_m 72°C (28 cycle). DNA products were quantified after polyacrylamide gel electrophoresis.

Image Analysis and Statistics

Autoradiographs were subjected to densitometric analysis (NIH Image 1.54). For each hepatic IGF-I mRNA species, the measurement of the optical density was obtained within a linear range by calibrating the exposure time for the autoradiographic films. The level of optical density was then corrected using the level of 18S rRNA in the same sample measured by the ethidium bromide–stained agarose gel used for the Northern blot (Fig. 3). The means and standard error of means (SEM) among genotypes were calculated and results were analyzed using one-way ANOVA. Age-related alterations, sex effects, and potential interactions between these factors were analyzed by Design of Experiment (DOE, release 14; Minitab Inc., PA) software.

Acknowledgments

This work is supported by the National Institute of Neurological Diseases and Stroke and the Riley Children Foundation.

References

1. Liu, J.-P., Baker, J., Perkins, A. S., Robertson, E. J., and Efstratiadis, A. (1993). *Cell* **75,** 59–72.
2. Baker, J., Liu, J.-P., Robertson, E. J., and Efstratiadis, A. (1993). *Cell* **75,** 73–82.
3. Mathews, L. S., Hammer, R. E., Brinster, R. L., and Palmiter, R. D. (1988). *Endocrinology* **123,** 433–437.
4. Mathews, L. S., Hammer, R. E., Behringer, R. R., et al. (1988). *Endocrinology* **123,** 2827–2833.
5. Coschigano, K. T., Holland, A. N., Riders, M. E., List, E. O., Flyvbjerg, A., and Kopchick, J. J. (2003). *Endocrinology* **144,** 3799–3810.
6. Palmiter, R. D., Brinster, R. L., Hammer, R. E., et al. (1982). *Nature* **300,** 611–615.
7. Palmiter, R. D., Norstedt, G., Gelinas, R. E., Hammer, R. E., and Brinster, R. L. (1983). *Science* **222,** 809–814.
8. D'Ercole, A. J., Ye, P., Calikoglu, A. S., and Gutierrez-Ospina, G. (1996). *Mol. Neurobiol.* **13,** 227–255.
9. Rakic, P. and Sidman, R. L. (1973). *Proc. Natl. Acad. Sci. USA* **70,** 240–244.
10. Smeyne, R. J. and Goldowitz, D. (1989). *J. Neurosci.* **9,** 1608–1620.
11. Lee, W.-H., Wang, G.-M., Lo, T., Triarhou, L. C., and Ghetti, B. (1995). *Brain Res. Mol. Brain Res.* **30,** 259–268.
12. Zhong, J., Deng, J., Ghetti, B., and Lee, W.-H. (2002). *J. Neurosci. Res.* **70,** 36–45.
13. Zhang, W., Ghetti, B., and Lee, W.-H. (1997). *Brain Res. Dev. Brain Res.* **98,** 164–176.
14. Ghetti, B., Alyea, C. J., and Muller, J. (1978). *J. Neuropathol. Exp. Neurol.* **37,** 617.
15. Torres-Aleman, I. (2000). *Mol. Neurobiol.* **21,** 153–160.
16. Busiguina, S., Fernanadez, S. C., Barrios, V., et al. (2000). *Neurobiol. Dis.* **7,** 657–665.
17. Fernandez, A. M., De la Vega, A. G., and Torres-Aleman, I. (1998). *Proc. Natl. Acad. Sci. USA* **95,** 1253–1258.
18. Clemmons, D. R. (1998). *Mol. Cellular Endocrinol.* **140,** 19–24.
19. Hossenlopp, P., Seurin, D., Segovia-Quinson, B., Hardouin, S., and Binoux, M. (1986). *Anal. Biochem.* **154,** 138–143.
20. Lane, P. W. (1964). *Mouse News Lett.* **30,** 32.
21. Sidman, R. L., Green, M. C., and Appel, S. H. (1965). *Catalog the neurological mutants of the mouse.* Harvard University Press, Cambridge, MA.
22. Caviness, V. S. and Rakic, P. (1978). *Ann. Rev. Neurosci.* **1,** 297–326.
23. Sekiguchi, M., Nowakowski, R. S., Nagato, Y., et al. (1995). *Brain Res.* **629,** 262–267.
24. Roffler-Tarlov, S., Martin, B., Graybiel, A. M., and Kauer, J. S. (1996). *J. Neurosci.* **16,** 1819–1826.
25. Mauras, N., Rogol, A. D., Haymond, M. W., and Veldhuis, J. D. (1996). *Horm. Res.* **45,** 74–80.
26. Metzger, D. L. and Kerrigan, J. R. (1994). *J. Clin. Endocrinol. Metab.* **79,** 513–518.
27. Schwartz, N. B., Szabo, M., Verina, T., et al. (1999). *Neuroendocrinology* **68,** 374–385.
28. Brinkmann, A. O., Blok, L. J., de Ruiter, P. E., et al. (1999). *J. Steroid Biochem. Mol. Biol.* **69,** 307–313.
29. Weissberger, A. J. and Ho, K. Y. (1993). *J. Clin. Endocrinol. Metab.* **76,** 1407–1412.
30. Urban, R. J., Bodenburg, Y. H., Gilkison, C., et al. (1995). *Am. J. Physiol. Endocrinol. Metab.* **269,** E820–E826.
31. Metzger, D. L. and Rogol, A. D. (1994). Proc. 76th Annu Meeting Endocr Soc, Anaheim, CA, abstract 522.
32. Veldhuis, J. D., Metzger, D. L., Martha, P. M. J., et al. (1997). *J. Clin. Endocrinol. Metab.* **82,** 3414–3420.
33. Mauras, N. and Beaufrere, B. (1995). *J. Clin. Endocrinol. Metab.* **80,** 869–874.
34. LeRoith, D., Scavo, L., and Butler, A. (2001). *Trends Endocrinol. Metabol.* **12,** 48–52.
35. Baxter, R. C. (2000). *Am. J. Physiol. (Endocrinol. Metab.)* **278,** E967–E976.
36. Jones, J. I. and Clemmons, D. R. (1995). *Endo. Rev.* **16,** 3–34.
37. Liu, J. L., Yakar, S., and LeRoith, D. (2000). *Proc. Soc. Exp. Biol. Med.* **223,** 344–351.
38. Liu, J. L., Yakar, S., and LeRoith, D. (2000). *Endocrinology* **141,** 4436–4441.
39. Yakar, S., Liu, J. L., Stannard, B., et al. (1999). *Proc. Natl. Acad. Sci. USA* **96,** 7324–7329.
40. Lesage, D., Duprat, F., Fink, M., et al. (1994). *FEBS Lett.* **353,** 27–42.
41. Patil, N., Cox, D. R., Bhat, D., Faham, M., Myers, R. M., and Peterson, A. S. (1995). *Nature Genet.* **11,** 126–129.
42. Slesinger, P. A., Patil, N., Liao, J., Jan, Y. N., Jan, L. Y., and Cox, D. R. (1996). *Neuron* **16,** 321–331.
43. Doré, S., Kar, S., Rowe, W., and Quirion, R. (1997). *Neuroscience* **80,** 1033–1040.
44. Chomczynski, P. and Sacchi, N. (1987). *Anal. Biochem.* **162,** 156–159.